

1 Impacts of the seasonal distribution of rainfall on vegetation productivity 2 across the Sahel

3 Wenmin Zhang^{a,b}, Martin Brandt^b, Xiaoye Tong^b, Qingjiu Tian^{a*}, Rasmus Fensholt^b

4 ^a *International Institute for Earth System Sciences, Nanjing University, 210023 Nanjing, China*

5 ^b *Department of Geosciences and Natural Resource Management, University of Copenhagen, 1350 Copenhagen,
6 Denmark*

7

8 **Abstract** Climate change in drylands has caused alterations in the seasonal distribution of rainfall including increased heavy
9 rainfall events, longer dry spells, and a shifted timing of the wet season. Yet, the aboveground net primary productivity (ANPP)
10 in drylands is usually explained by annual rainfall sums, disregarding the influence of the seasonal distribution of rainfall. This
11 study tested the importance of rainfall metrics in the wet season (onset and cessation of the wet season, number of rainy days,
12 rainfall intensity, number of consecutive dry days and heavy rainfall events) on growing season ANPP. We focused on the
13 Sahel and north-Sudanian region (100–800 mm yr⁻¹) and applied daily satellite based rainfall estimates (CHIRPS v2.0) and
14 growing season integrated NDVI (MODIS) as a proxy for ANPP over the study period 2001–2015. Growing season ANPP in
15 the arid zone (100–300 mm yr⁻¹) was found to be rather insensitive to variations in the seasonal rainfall metrics, whereas
16 vegetation in the semi-arid zone (300–700 mm yr⁻¹) was significantly impacted by most metrics, especially by the number of
17 rainy days and timing (onset and cessation) of the wet season. We analyzed critical breakpoints for all metrics to test if
18 vegetation response to changes in a given rainfall metric surpasses a threshold beyond which vegetation functioning is
19 significantly altered. It was shown that growing season ANPP was particularly negatively impacted after >14 consecutive dry
20 days and that a rainfall intensity of ~13 mm day⁻¹ was detected for optimum growing season ANPP. We conclude that number

* Corresponding author at: Kunshan Building Xianlin avenue, 163#, Nanjing, China

E-mail address: tianqj@nju.edu.cn (Q.Tian).

21 of rainy days and the timing of the wet season are seasonal rainfall metrics being decisive for favorable vegetation growth in
22 semi-arid Sahel which needs to be considered when modelling primary productivity from rainfall in the drylands of Sahel and
23 elsewhere.

24 **Keywords:** Drylands, Seasonal rainfall metrics, Aboveground net primary production, Remote sensing

25

26 **1 Introduction**

27 Livihoods in most drylands depend heavily on aboveground net primary production (ANPP) in the form of
28 rain-fed crops and fodder for livestock (Abdi et al., 2014; Leisinger and Schmitt, 1995). Annual ANPP thus plays
29 a decisive role in the context of livelihood strategies, food security and people's general wellbeing. ANPP in
30 drylands is primarily controlled by water availability with annual rainfall typically being limited to a short and
31 erratic wet season which can be highly variable in time and space. The current study focuses on the sub-Saharan
32 Sahel zone which is one of the largest dryland areas in the world. The Sahel has been referred to as the region
33 showing the largest rainfall anomalies worldwide during the last century (Nicholson, 2000). Throughout the
34 centuries, the Sahelian population has adapted to this high rainfall variability and the associated great inter-annual
35 differences in available ANPP are balanced for example by a temporary abandonment of agriculture or seasonal
36 livestock migration (Romankiewicz et al., 2016). However, 21st century climate change is predicted to threaten
37 established coping strategies; not only by increasing inter-annual variability of rainfall regimes as a whole (Field,
38 2012; Kharin et al., 2007), but also by an increasingly unpredictable seasonality and an altered number of heavy
39 rainfall and drought events (Fischer et al., 2013; Smith, 2011; Taylor et al., 2017). Improved knowledge on the
40 vegetation response to the seasonal variability of rainfall is thus crucial to better interpret the consequences of
41 climate predictions of an altered global hydrological cycle and to implement appropriate adaptation measures to
42 climate change and food security in arid and semi-arid lands like the Sahel.

43 While it is well known that the productivity of dryland vegetation is highly prone to variations in the
44 availability of water resources at the annual scale (Fensholt et al., 2013; Fensholt and Kjeld, 2011; Herrmann et al.,
45 2005; Huber et al., 2011), there is a current lack of understanding how the seasonal distribution of rainfall impacts
46 on growing season ANPP (Rishmawi et al., 2016). Several studies have demonstrated the vegetation sensitivity to
47 the timing and magnitude of rainfall events based on individual plot data and model estimates (Bates et al., 2006;
48 Fay et al., 2000; Guan et al., 2014; Thomey et al., 2011), but the impact of specific rainfall metrics (such as wet
49 season length/timing, number of rainy days, rainfall intensity, number of consecutive dry days and extreme events)
50 on dryland vegetation productivity has rarely been studied in spatially distributed manner, potentially including
51 different biotic and abiotic controls. A few studies show that there is a strong dependency of Sahelian vegetation
52 growth on the timing of the wet season (Diouf et al., 2016) and the frequency and distribution of dry spells (Proud
53 and Rasmussen, 2011), but currently no regional scale study have systematically analyzed the importance of a
54 variety rainfall metrics on vegetation growth as a function of mean annual rainfall. Further, there is evidence
55 showing that not only a shift in the timing of the wet season but also increasing extreme events occur in Sahel
56 (Panthou et al., 2014; Sanogo et al., 2015; Taylor et al., 2017; Zhang et al., 2017), suggesting the need for a
57 comprehensive understanding on how rainfall seasonality impacts on vegetation production.

58 The assessment of rainfall metrics capturing the seasonal variability and the associated impact on growing
59 season ANPP requires daily rainfall records and a robust methodology being able to extract the timing (onset and
60 cessation) and duration of the wet season (Dunning et al., 2016; Liebmann et al., 2012). The availability and quality
61 of such data, and uncertainties in methods to extract the rainfall seasonality have complicated regionally scaled
62 studies on this topic (Fitzpatrick et al., 2015). However, a new generation of high spatial resolution satellite based
63 daily rainfall estimates blended with station data has recently opened up the possibility to fill the gap between plot
64 and model based studies. Here our study aims at applying daily rainfall estimates to analyze and understand the
65 impact of seasonal rainfall metrics on vegetation productivity for the entire Sahel.

66 **2 Materials and methods**

67 An empirical analysis was conducted based on gridded information of rainfall metrics based on daily satellite
68 estimates and seasonally integrated NDVI (hereafter \sum NDVI) as a proxy for the growing season ANPP. The period
69 of analysis covers 2001–2015 which allows for a per-pixel analysis including state of the art Earth observation
70 datasets of both Climate Hazards Group InfraRed Precipitation with Station (CHIRPS v2.0) and Moderate
71 Resolution Imaging Spectroradiometer (MODIS) vegetation. The rainfall metrics include: number of rainy days,
72 daily intensity, heavy rainfall events, number of consecutive dry days and seasonal rainfall amount which were
73 analyzed as explanatory variables for the observed spatial variability in seasonal vegetation productivity along the
74 gradient of mean seasonal rainfall.

75

76 **2.1 Study area**

77 The Sahelian zone covers arid and semi-arid biomes and is one of the world's largest dryland areas bordering
78 the Sahara Desert to the north (Fig. 1). The delineation of the Sahel is often done by using average annual rainfall
79 isohyets, with the northern boundary at 100 mm yr⁻¹ and the southern boundary defined by 700 mm yr⁻¹ (Lebel and
80 Ali, 2009). For this study we expanded the southern limit towards the Sudanian zone until 800 mm yr⁻¹ to include
81 also the zone where rainfall as the primary climatic forcing variable on vegetation productivity is expected to level
82 off (Fensholt et al., 2013; Huber et al., 2011; Kaspersen et al., 2011). The Sahel is characterized by a unimodal
83 rainfall regime and the landscape is generally flat and consists of large plains interspersed with sand dunes and
84 rocky formations. The large stretches of plains are mainly used for grazing and subsistence cultivation. The northern
85 parts of the Sahel are dominated by open and sparse grass- and shrublands, while cropland, open woody vegetation
86 and deciduous shrublands characterize the southern parts (Breman and Kessler, 1995).

87

88 2.2 CHIRPS rainfall data

89 The CHIRPS v2.0 data set uses TIR (Thermal InfraRed) imager and gauge data, as well as monthly precipitation
90 climatology, CHPClim, and atmospherically modelled rainfall fields from the NOAA Climate Forecast System,
91 version 2 (CFSv2) and TRMM 3B42 (Funk et al., 2015). The CHIRPS data are provided as grids at 0.05° and 0.25°
92 spatial resolutions and extends from 1981 to present. In our study, the CHIRPS data at daily resolution with a
93 spatial resolution of 0.05° were used to extract seasonal rainfall metrics.

94

95 2.3 Deriving seasonal rainfall metrics

96 The method used to identify the onset and cessation of the wet season is referred to Liebmann et al. (2012)
97 and applicable to multiple datasets for precipitation seasonality analysis across the African continent (Dunning et
98 al., 2016). As was described in Liebmann et al. (2012), the climatology wet season was initially determined by
99 the climatological cumulative daily rainfall anomaly, $A(d)$, calculated from the long-term (2001–2015) average
100 rainfall (R_i) for each day of the calendar year minus the long-term annual-mean daily average (\bar{R}). The day with
101 minimum value (d_s) was defined as the start of the wet season and the maximum point (d_c) marks the end of the
102 wet season.

103

$$104 \quad (d) = \sum_{i=1}^d R_i - \bar{R} \quad (1)$$

105 Subsequently, the onset and cessation were calculated individually for each year and each grid point. For each
106 year the extraction of the rainfall metrics of the wet season was based on equation (2). The daily cumulative
107 rainfall anomaly $A(D)$ on a certain day (P_i) was computed for each day in the range $d_s - 50$ to $d_c + 50$ for each year
108 and the day with minimum value was considered as the onset of the wet season.

109

$$(D) = \sum_{j=d_s-50}^D P_i - \bar{R} \quad (2)$$

Once the onset and cessation dates of the wet season for each year were found, the remaining metrics were calculated (Table 1). Figure 2a illustrated an example of daily rainfall for the grid point (13.5° N, 5.0° W) in 2001 and the corresponding cumulative daily anomaly curves were shown in Figure 2b. The blue and red lines signify $A(d)$ and $A(D)$, respectively. The range of minimum and maximum points in the blue line denoted the climatological wet season (Liebmann et al., 2012). The wet season of each individual year was then determined based on the daily precipitation observations covered by the climatological wet season. Areas where the annual minimum occurs after the 1st of October (desert areas) were excluded from further analysis (Diaconescu et al., 2015).

2.4 Estimation of growing season ANPP

The MODIS/Terra surface reflectance product (MOD09Q1, collection 6) was used to derive a time series of NDVI for the period 2001–2015. NDVI was calculated from the MODIS red and near-infra red bands (8 day composites). The growing season integrated NDVI (\sum NDVI) was used as a proxy for the growing season ANPP. The method was well established and proven to be a reliable proxy for the growing season ANPP in Sahel (Fensholt et al., 2013; Olsson et al., 2005). The \sum NDVI (defined by the area under the curve delimited by start and end of the season) was derived using the TIMESAT software (Jönsson and Eklundh, 2004), which was a widely used tool to extract vegetation seasonal metrics. For this study, we applied the Savitzky-Golay filter implemented in TIMESAT with the following settings: A window size of four was applied and a seasonal parameter of 0.5 to fit one season per year. Both the number of iterations for upper envelope adaptation and strength of the envelope adaptation were set to two and the start and end of season were determined as 20% and 50% of the amplitude respectively. The \sum NDVI data was then aggregated to the spatial resolution of CHIRPS

132 (0.05°) using a bilinear resampling method. Both Globeland30 (Chen et al., 2014) and ESA CCI (2010) land
133 cover maps (<https://www.esa-landcover-cci.org/>) were used to mask water bodies, irrigated and flooded areas if
134 one or both of the land cover products indicated the presence of water in a pixel.

135

136 **2.5 Statistical analyses**

137 An exponential regression was used to quantify the relationship between growing season ANPP and seasonal
138 rainfall metrics for the entire study area (Fig. 5) and the non-parametric Spearman's rank correlation coefficient
139 was used to measure the relationship between growing season ANPP and seasonal rainfall metrics as a function of
140 seasonal rainfall amount (Fig. 6). Additionally, Generalized Additive Models (GAMs) implemented using the
141 MGCV package (Wood, 2017) in the *R* computing environment (*R* Team, 2014) were applied to derive smooth
142 response curves with seasonal rainfall amount as the explanatory variable and the linear coefficients (averaged over
143 10 mm rainfall steps) as the response variable (Fig. 7). The models were parameterized assuming normal error
144 distributions. Furthermore, a random forest ensemble learning method (Breiman, 2001) was used to analyze the
145 relative importance of individual seasonal rainfall metrics on growing season ANPP as a function of the seasonal
146 rainfall amount (Fig. 8a). This algorithm produces multiple decision trees based on bootstrapped samples and the
147 nodes of each tree are built up by an iterative process of choosing and splitting nodes to achieve maximum variance
148 reduction. Thus the metrics with highest difference are considered as the most important factors. All pixels based
149 on 15 year averages of seasonal rainfall metrics and ANPP were used for this analysis. Additionally, a multiple
150 regression analysis was applied to identify and map the spatial distribution of the relative importance of the three
151 most important seasonal rainfall metrics (onset and cessation of the wet season and rainy days) explaining the
152 growing season ANPP at the per-pixel level (based on a 15 year time series) (Fig. 8b).

153 A piecewise regression was used to identify breakpoints (Muggeo, 2003), i.e. critical thresholds in the
154 relationship between rainfall metrics and vegetation growth (Fig. 9). A breakpoint is an indication that the

155 vegetation response to changes in a given rainfall metric surpasses a threshold beyond which vegetation functioning
156 is significantly altered. Such a threshold, at the level of individual rainfall seasonality metric, provides an indication
157 of rainfall conditions beyond which vegetation does not tolerate further stress without a marked impact on the
158 growing season ANPP. The 95th percentile of \sum NDVI was selected to represent the potential vegetation
159 productivity attainable for a given seasonal rainfall metric (Donohue et al., 2013). Seasonal rainfall metrics were
160 binned according to the dynamic range of the individual metrics and the average 95th percentile of \sum NDVI was
161 calculated for each bin (for onset, cessation and RD bins with an interval of one were used; for SDII a bin of 0.3
162 was applied; for R95sum bin intervals were set to 0.02; finally we used bins of 0.5 for CDD). The breakpoint
163 regression was then applied to the potential vegetation productivity and corresponding seasonal rainfall metrics.

164

165 **2.6 Data availability**

166 The CHIRPS data are available at <http://chg.geog.ucsb.edu/data/chirps/>. The MODIS surface Reflectance product
167 (MOD09Q1) can be downloaded at https://lpdaac.usgs.gov/dataset_discovery/modis/modis_products_table. The
168 global land cover 30 is available at <http://www.globeland30.org/> and ESA CCI land cover is accessed from
169 <https://www.esa-landcover-cci.org/>.

170

171 **3 Results**

172 **3.1 Spatial pattern of seasonal rainfall metrics**

173 A clear north-south gradient was observed for the onset, rainy days (RD), heavy rainfall events (R95sum) and
174 consecutive dry days (CDD) based on a 15 year (2001–2015) average value, with an earlier onset, more rainy days
175 and less heavy rainfall events towards the south (Fig. 3a, c, e). The cessation of the wet season (Fig. 3b) showed
176 some longitudinal differences with the latest dates found in the eastern Sahel, followed by the western Sahel and
177 the central Sahel showing the earliest cessation dates. A considerable difference between southeastern and

178 southwestern Sahel (Fig. 3d) was observed in the rainfall intensity (SDII). The relatively low rainfall intensity in
179 the southeastern Sahel was mirrored by considerably higher numbers of rainy days.

180

181 **3.2 General response of growing season ANPP to rainfall metrics**

182 The median growing season ANPP clearly followed the mean seasonal rainfall gradient (Fig. 4) with other
183 biotic and abiotic factors (e.g. soil texture, nutrients, species composition, fire regime and seasonal rainfall
184 distribution) causing a wide range of values as indicated by the different quantile values.

185 The relationships between all the rainfall metrics and growing season ANPP were found to be significant
186 ($p < 0.001$) and the coefficient of determination (r^2) modelled by exponential regression varied between 0.27 and
187 0.73 (Fig. 5). For the region as a whole, the number of rainy days was identified as the most important metric
188 impacting on the growing season ANPP ($r^2 = 0.73$) (Fig. 5c), closely followed by heavy rainfall events (R95sum)
189 ($r^2 = 0.72$) (Fig. 5e), consecutive dry days (CDD) ($r^2 = 0.54$) (Fig. 5f) and cessation ($r^2 = 0.37$) (Fig. 5b) of the wet
190 season. The impact of the onset on growing season ANPP was also relatively strong ($r^2 = 0.47$) (Fig. 5a), whereas
191 a rather weak relationship was observed between growing season ANPP and rainfall intensity (SDII) ($r^2 = 0.27$)
192 (Fig. 5d). For all seasonal rainfall metrics except RD, R95sum and CCD, the plots showed some signs of a bimodal
193 distribution of the points, which was caused by the differences in the east-west patterns of the spatial distribution
194 of seasonal rainfall metrics (onset, cessation and SDII) in Sahel as reported in Figure 3.

195

196 **3.3 Response of growing season ANPP to seasonal rainfall metrics along the rainfall gradient**

197 Although the relationship between growing season ANPP and seasonal rainfall amount (R) obviously changed
198 along the rainfall gradient (Fig. 4), variations in seasonal rainfall distribution (e.g., onset and R95sum) can cause
199 considerable changes in growing season ANPP under the same rainfall gradient (Fig. 5). The influence of seasonal
200 rainfall distribution on growing season ANPP was thus analyzed under different mean annual rainfall values along

201 the north (low rainfall) to south (high rainfall) gradient (Fig. 6). The dependency of growing season ANPP on
202 seasonal rainfall metrics was clearly seen to be a function of the seasonal rainfall amount. Below ~ 300 mm yr⁻¹,
203 the vegetation seems to be stable and rather insensitive to variations of the rainfall metrics, however, above 300
204 mm yr⁻¹, the impacts can be clearly seen by a larger spread in growing season ANPP values for a given amount of
205 seasonal rainfall (Fig. 6). For example, the growing season ANPP decreased strongly with a later onset, an earlier
206 cessation of the wet season, a smaller number of rainy days, a higher rainfall intensity, more heavy rainfall events
207 and longer dry spells. Above ~ 700 mm yr⁻¹, the vegetation showed again a reduced sensitivity to variations of the
208 wet season by a convergence of growing season ANPP values irrespective of the seasonal rainfall metric value.

209 The non-parametric Spearman's rank correlation coefficient was used to quantify the strength of the impact
210 of individual seasonal rainfall metrics on growing season ANPP as a function of seasonal rainfall (Fig. 7). In general,
211 the impacts of rainfall metrics on vegetation were distinctive along the 100–800 mm yr⁻¹ gradient with a peak in r
212 values (respectively positive or negative dependent on the rainfall metric) for most metrics around 650 mm yr⁻¹
213 followed by a sharp drop-off (Fig. 7). It should be noted that modelling uncertainties increased for all rainfall
214 metrics due to fewer observations in the lowermost seasonal rainfall total bins. For the wet season the pattern of
215 RD, SDII, R95sum and CDD showed a sharp decrease in r values from 100–300 mm yr⁻¹. The number of
216 consecutive dry days (CDD) showed moderate r values balancing around zero generally indicating less importance
217 of the CDD variable on growing season ANPP along the rainfall gradient analyzed.

218 The relative importance of the individual rainfall metrics on growing season ANPP was assessed based on a
219 random forest model (Fig. 8a). The explained variance of growing season ANPP explained by rainfall metrics (blue
220 line in Fig. 8a) was increasing with mean annual rainfall up to 600–700 mm yr⁻¹ from where the degree of explained
221 variance decreases, which corresponds with the results presented in Figure 4 (the widest belt of the quantile values
222 was observed for rainfall of 600–700 mm yr⁻¹, suggesting that the seasonal rainfall metrics additional to the seasonal
223 rainfall amount was increasingly important in this rainfall zone) and in Figure 7. The cessation of the wet season

224 was identified as the most important factor controlling growing season ANPP in semi-arid areas of Sahel (400–700
225 mm yr⁻¹), followed by the onset and number of rainy days. As measured by the relative importance, these three
226 rainfall metrics together accounted for 60–70% of the variance explained by all rainfall metrics for all seasonal
227 rainfall amounts. In arid areas (100–300 mm yr⁻¹) the number of rainy days was found to be the most important
228 variable.

229 The spatial distribution of the relative importance of the onset and cessation of the wet season and number of
230 rainy days on growing season ANPP was identified at the pixel-level for 2001 to 2015 (Fig. 8b). At Sahel scale,
231 the number of rainy days (bluish colors) was observed to be the dominating factor, followed by the onset of the wet
232 season (reddish colors) and cessation (greenish colors). There were no clear signs of a latitudinal or longitudinal
233 dependency on which rainfall metric was dominating, but some clustering was evident with a predominance of
234 rainy days influence in the Western Sahel with limited influence by the cessation date on the growing season ANPP.

235

236 **3.4 Critical points for growing season ANPP**

237 A piecewise regression between growing season ANPP and seasonal rainfall metrics was applied to identify
238 if critical breakpoints in the relationship between growing season ANPP and rainfall metrics exist (Fig. 9). We
239 found that the most evident thresholds (average values for the Sahel zone) in relation to seasonal rainfall metrics
240 influence on growing season ANPP relate to the onset of the wet season (Fig. 9a), the rainfall intensity (SDII) (Fig.
241 9d) and consecutive dry days (CDD) (Fig. 9f). If the onset of the wet season was later than day of year 140 this
242 will have an increasingly negative effect on growing season ANPP as a function of the onset delay and contrastingly
243 if the onset starts earlier than day of year 140 this will also have an increasingly adverse effect on growing season
244 ANPP. Also, an optimum of rainfall intensity of 13 mm day⁻¹ was detected; if rainfall intensity exceeds 13 mm day⁻¹,
245 vegetation productivity starts to be negatively affected, whereas a lower intensity will also negatively impact on
246 growing season ANPP. There was a pronounced decline in growing season ANPP as a function of number of

247 consecutive dry days. However, when CDD exceeds ~14 days a breakpoint in the curve was detected, as dry spells
248 of this magnitude led to a strong reduction in vegetation growth. The number of rainy days (Fig. 9c) was linearly
249 related to growing season ANPP until 69 days, beyond which RD became less decisive for the amount of growing
250 season ANPP. Similarly, heavy rainfall events (fraction of annual rainfall events exceeding the 95th percentile)
251 (Fig. 9e) were negatively related to growing season ANPP, until a certain threshold (larger than 0.80), from where
252 the vegetation loses sensitivity to the impact from an increased frequency of heavy rainfall events. Finally, the
253 cessation date of the wet season (Fig. 9b) was shown to be nearly linearly related to growing season ANPP. A
254 breakpoint was detected by the piecewise regression algorithm around day 285, beyond which the delay in cessation
255 date was slightly more favorable for higher growing season ANPP yields as compared to a cessation date before
256 day 285.

257

258 **4 Discussion**

259 This study presents first empirical evidence on the impact of rainfall seasonality on vegetation productivity at
260 regional scale and the results provide a clear picture on the importance of six seasonal rainfall metrics on growing
261 season ANPP under different rainfall conditions (i.e. mean annual rainfall). Uncertainty in the rainfall data is
262 inevitably to have an impact on the extraction of seasonal rainfall metrics which further impacts the relationship
263 between seasonal rainfall metrics and ANPP. Based on improved climatologies systematic bias in the CHIRPS
264 dataset has been removed and the data is considered state-of-the-art within quasi-global, high spatial resolution
265 rainfall datasets (Funk et al., 2015). As this study does not address temporal changes in the seasonal rainfall metrics
266 or \sum NDVI, but merely presents results on the general coupling between rainfall metrics and vegetation productivity,
267 we consider the results to be statistically robust. We conducted a parallel set of analyses based on the RFE-2.0
268 rainfall product developed by the NOAA Climate Prediction Center (CPC) (Herman et al., 1997), which, like
269 CHIRPS, is also a gauge-satellite blended and the outcome of these analyses (not shown) yielded nearly similar

270 results as to what was presented here. At the same time \sum NDVI derived from MODIS will also be impacted from
271 cloud cover during the growing season, but the use of the Savitzky-Golay filtering algorithm has proven to be an
272 effective way of overcoming residual noise effects in the NDVI time-series (Fensholt et al., 2015).

273 The Sahel zone is often defined from isohyets of annual rainfall as a common denominator of the hydrological
274 conditions of the region. It was however shown here, that considerable east-west differences occurred in several of
275 the seasonal rainfall metrics analyzed with a much higher number of rainy days and corresponding lower rainfall
276 intensity in the southeastern Sahel as compared to the southwestern part. Variability in the rainfall intensity was
277 shown here to influence the growing season ANPP generated over a growing season (Fig. 9d) and hence spatio-
278 temporal changes in rainfall intensity (but characterized by the same amount of seasonal rainfall) will impact
279 vegetation productivity. This has important implications for the use of the rain use efficiency (RUE) (Houerou,
280 1984) or Residual Trend Analysis (RESTREND) approach (regressing \sum NDVI from annual precipitation and
281 subsequently calculating the residuals as the difference between observed \sum NDVI and \sum NDVI as predicted from
282 annual precipitation) (Evans and Geerken, 2004), which is derived from annually or seasonally summed rainfall
283 and commonly used as an indicator for land degradation (Archer, 2004; Bai et al., 2008; Fensholt and Kjeld, 2011;
284 Prince et al., 1998; Ratzmann et al., 2016; Wessels et al., 2007) as discussed in Ratzmann et al. (2016). Interestingly,
285 a limited impact of rainfall seasonality on growing season ANPP was found in arid lands below 300 mm yr⁻¹ rainfall,
286 suggesting that the species composition was adapted to rainfall variation, and that the rather sparse vegetation cover
287 was able to effectively utilize rainfall independent of the seasonal distribution. This was very different in the semi-
288 arid and northern sub-humid zone (300–700 mm yr⁻¹), where variations in rainfall seasonality were found to be
289 more closely linked with variations in growing season ANPP. This implied that a favorable distribution of rainfall
290 may lead to increased productivity, as it was observed in Senegal between 2006 and 2011 (Brandt et al., 2017), but
291 below average rainfall conditions with an unfavorable distribution led to an immediate reduction in vegetation
292 cover and growing season ANPP.

293 Not surprisingly, the number of rainy days showed the highest relationship with growing season ANPP (Fig.
294 5c), with increasing productivity along with increasing rainy days, up to 69 days, where the relation weakens (Fig.
295 9c). The importance of this metric was closely followed by the heavy rainfall events, which were negatively
296 correlated with growing season ANPP (Fig. 5e), and decreases the productivity until heavy rainfall events reached
297 a share of 80%, which led to a constant level of low vegetation productivity (Fig. 9e). The importance of the timing
298 of the wet season, i.e. the onset and cessation, increases rapidly along the rainfall gradient, having the highest
299 impact on growing season ANPP in the semi-arid zone (300–700 mm yr⁻¹). The reason for the importance of the
300 timing of the onset of the growing season on the growing season ANPP (Fig. 9a) with an almost linear decrease in
301 growing season ANPP as a function of onset delay should be found in the predominance of annual grasses which
302 are photoperiodic (Penning de Vries and Djiteye, 1982). The cessation of season was thus controlled by day length
303 and do therefore not compensate for a delay in the onset. Also, a too early onset was found to decrease growing
304 season ANPP, which is likely to be associated with so-called “false starts” of the growing season. Often, an early
305 start of the growing season is accompanied by a significant number of dry-days occurring shortly after the start of
306 the wet season with a detrimental impact upon plant growth (Proud and Rasmussen, 2011). Finally, we found that
307 the general impact of consecutive dry days was difficult to quantify (Fig. 7f). However, a rather clear critical
308 threshold of 14 consecutive days without rainfall was found to have an increased adverse impact on the growing
309 season ANPP. This threshold of 14 days as an average for Sahel was related to the depletion time of the upper layer
310 soil water and the root depth of the herbaceous stratum (primarily annual grasses) but will vary spatially with
311 different soil and vegetation types (Penning de Vries and Djiteye, 1982).

312 Several studies have reported a tendency towards an earlier start of the wet season (Sanogo et al., 2015; Zhang
313 et al., 2017), but projections predict a delay of the wet season in the later 21th century (Biasutti and Sobel, 2009;
314 Guan et al., 2014). Moreover, an increase in heavy rainfall events and prolonged dry spells were observed and
315 projected for the future (Sanogo et al., 2015; Taylor et al., 2017; Zhang et al., 2017). Our results showed that the

316 semi-arid zone will be most prone to these projected changes, and an increase in heavy rainfall events, a delay in
317 the onset of the wet season and dry spells exceeding 14 days will cause a significant reduction in vegetation
318 productivity, although the annual rainfall amount may be constant or even increasing. Disregarding the importance
319 and impact of varying rainfall distribution on vegetation productivity leads to a bias in any ANPP prediction, and
320 this knowledge should be implemented in any prediction and estimation of ANPP, both for ecosystem models and
321 remote sensing based analyses, especially in the context of food security. Although this study did not include a
322 temporal change component of the metrics analyzed, the length of high quality time series data of both vegetation
323 productivity and rainfall with a daily temporal resolution does provide the possibility for adding a temporal
324 dimension which will be pursued in a future study.

325

326 **5 Summary and conclusion**

327 In this study we analyzed the impact of seasonal rainfall distribution (represented by onset and cessation of the
328 wet season, number of rainy days, rainfall intensity, number of consecutive dry days and heavy rainfall events) on
329 growing season ANPP for the Sahelian zone. Overall, a clear north-south gradient was observed for the onset, rainy
330 days, heavy rainfall events and consecutive dry days, but also considerable differences in cessation date, number
331 of rainy days and the rainfall intensity were observed between Eastern and Western Sahel. We found the strongest
332 relationship between growing season ANPP and the number of rainy days ($r^2 = 0.73$), closely followed by a
333 relationship between growing season ANPP and heavy rainfall events ($r^2 = 0.72$). Growing season ANPP in the
334 arid zone (100–300 mm yr⁻¹) was rather insensitive to variations in the seasonal rainfall metrics, whereas vegetation
335 in the semi-arid zone (300–700 mm yr⁻¹) was significantly impacted by most metrics, especially by the number of
336 rainy days and timing (onset and cessation) of the wet season. Finally, the critical breakpoints analysis between
337 growing season ANPP and all rainfall metrics showed that the growing season ANPP were particularly negatively
338 impacted after >14 consecutive dry days and that a rainfall intensity of 13 mm day⁻¹ was detected for optimum

339 growing season ANPP. Overall, it can be concluded that seasonal rainfall distribution significantly influence ANPP
340 and the effect of different rainfall metrics was observed to vary along the north-south rainfall gradient. These
341 findings have important implications for the sheer amount of dryland studies in which annually or seasonally
342 summed rainfall and ANPP are used to derive indicators of land degradation or anthropogenic influence (e.g. the
343 use of RUE and RESTREND). When studying subtle changes in dryland vegetation productivity based on time
344 series of satellite data, as caused by both climate and anthropogenic forcing, it is essential also to consider the
345 potential effect from changes in the rainfall regime as expressed in the seasonal rainfall metrics studied here. Inter-
346 annual differences in the seasonal distribution of rainfall is known to have an impact on species composition in
347 Sahel (Mbow et al., 2013) and it is likely that the herbaceous vegetation is able to adapt to changes seasonal rainfall
348 distribution expressed by a shift in the abundance of species favored by increased heavy rainfall events and longer
349 dry spells.

350

351 *Competing interests.* The authors declare that they have no conflict of interest.

352

353 *Acknowledgements.* This study is jointly supported by the European Union's Horizon 2020 research and
354 innovation programme under the Marie Skłodowska-Curie grant agreement (project BICSA number 656564),
355 China Scholarship Council (CSC, 201506190076), and the Danish Council for Independent Research (DFF)
356 project: Greening of drylands: Towards understanding ecosystem functioning changes, drivers and impacts on
357 livelihoods, and Chinese National Science and Technology Major Project (03-Y20A04-9001-15/16). Also, we
358 would like to thank the associate editor Jochen Schöngart, the reviewer M.Marshall and the anonymous reviewer
359 for providing detailed comments and constructive suggestions.

360

361 **Reference**

362 Abdi, A. M., Seaquist, J., Tenenbaum, D. E., Eklundh, L. and Ardö, J.: The supply and demand of net primary
363 production in the Sahel, *Environmental Research Letters*, 9(9), 94003, doi:10.1088/1748-9326/9/9/094003, 2014.

364 Archer, E.: Beyond the “climate versus grazing” impasse: using remote sensing to investigate the effects of
365 grazing system choice on vegetation cover in the eastern, *Journal of Arid Environments*, 57(3), 381–408,
366 doi:10.1016/S0140-1963(03)00107-1, 2004.

367 Bai, Z., Dent, D. and Olsson, L.: Proxy global assessment of land degradation, *Soil use and Management*, 24,
368 223–234, doi:10.1111/j.1475-2743.2008.00169.x, 2008.

369 Bates, J. D., Svejcar, T., Miller, R. F. and Angell, R. A.: The effects of precipitation timing on sagebrush
370 steppe vegetation, *Journal of Arid Environments*, 64(4), 670–697, doi:10.1016/j.jaridenv.2005.06.026, 2006.

371 Biasutti, M. and Sobel, A. H.: Delayed Sahel rainfall and global seasonal cycle in a warmer climate,
372 *Geophysical Research Letters*, 36(23), 1–5, doi:10.1029/2009GL041303, 2009.

373 Brandt, M., Tappan, G., Diouf, A., Beye, G. and Mbow, C.: Woody vegetation die off and regeneration in
374 response to rainfall variability in the West African Sahel, *Remote Sensing*, 9, 39, doi:10.3390/rs9010039, 2017.

375 Breiman, L.: Random forests, *Machine Learning*, 45(1), 5–32, doi:10.1023/A:1010933404324, 2001.

376 Breman, H. and Kessler, J.: *Woody Plants in Agro-Ecosystems of Semi-Arid Regions: with an Emphasis on*
377 *the Sahelian Countries*, Springer Berlin Heidelberg, 1995.

378 Chen, J., Chen, J., Liao, A., Cao, X., Chen, L., Chen, X., He, C., Han, G., Peng, S., Lu, M., Zhang, W., Tong,
379 X. and Mills, J.: Global land cover mapping at 30 m resolution: A POK-based operational approach, *ISPRS*
380 *Journal of Photogrammetry and Remote Sensing*, 103, 7–27, doi:10.1016/j.isprsjprs.2014.09.002, 2014.

381 Diaconescu, E. P., Gachon, P., Scinocca, J. and Laprise, R.: Evaluation of daily precipitation statistics and
382 monsoon onset/retreat over western Sahel in multiple data sets, *Climate Dynamics*, 45(5–6), 1325–1354,
383 doi:10.1007/s00382-014-2383-2, 2015.

384 Diouf, A. A., Hiernaux, P., Brandt, M., Faye, G., Djaby, B., Diop, M. B., Ndione, J. A. and Tychon, B.: Do
385 agrometeorological data improve optical satellite-based estimations of the herbaceous yield in Sahelian semi-arid
386 ecosystems?, *Remote Sensing*, 8(8), 668, doi:10.3390/rs8080668, 2016.

387 Donohue, R. J., Roderick, M. L., McVicar, T. R. and Farquhar, G. D.: Impact of CO₂ fertilization on
388 maximum foliage cover across the globe's warm, arid environments, *Geophysical Research Letters*, 40(12),
389 3031–3035, doi:10.1002/grl.50563, 2013.

390 Dunning, C. M., Black, E. C. L. and Allan, R. P.: The onset and cessation of seasonal rainfall over Africa,
391 *Journal of Geophysical Research: Atmospheres*, 121, 11,405–11,424, doi:10.1002/2016JD025428, 2016.

392 Evans, J. and Geerken, R.: Discrimination between climate and human-induced dryland degradation, *Journal*
393 *of Arid Environments*, 57(4), 535–554, doi:10.1016/S0140-1963(03)00121-6, 2004.

394 Fay, P. A., Carlisle, J. D., Knapp, A. K., Blair, J. M. and Collins, S. L.: Altering rainfall timing and quantity in
395 a mesic grassland ecosystem: Design and performance of rainfall manipulation shelters, *Ecosystems*, 3(3), 308–
396 319, doi:10.1007/s100210000028, 2000.

397 Fensholt, R. and Kjeld, R.: Analysis of trends in the Sahelian “rain-use efficiency” using GIMMS NDVI, RFE
398 and GPCP rainfall data, *Remote Sensing of Environment*, 115(2), 438–451, doi:10.1016/j.rse.2010.09.014, 2011.

399 Fensholt, R., Rasmussen, K., Kaspersen, P., Huber, S., Horion, S. and Swinnen, E.: Assessing land
400 degradation/recovery in the African Sahel from long-term earth observation based primary productivity and
401 precipitation relationships, *Remote Sensing*, 5(2), 664–686, doi:10.3390/rs5020664, 2013.

402 Fensholt, R., Horion, S., Tagesson, T., Ehammer, A., Grogan, K., Tian, F., Huber, S., Verbesselt, J., Prince, S.
403 P., Tucker, C. J. and Rasmussen, K.: Assessment of Vegetation Trends in Drylands from Time Series of Earth
404 Observation Data, *Remote Sensing Time Series*, 2015.

405 Field, C.: Managing the risks of extreme events and disasters to advance climate change adaptation, IPCC
406 special report of the intergovernmental panel on climate change, 2012.

407 Fischer, E. M., Beyerle, U. and Knutti, R.: Robust spatially aggregated projections of climate extremes,
408 *Nature Climate Change*, 3(12), 1033–1038, doi:10.1038/nclimate2051, 2013.

409 Fitzpatrick, R. G. J., Bain, C. L., Knippertz, P., Marsham, J. H. and Parker, D. J.: The West African monsoon
410 onset: A concise comparison of definitions, *Journal of Climate*, 28(22), 8673–8694, doi:10.1175/JCLI-D-15-
411 0265.1, 2015.

412 Funk, C., Peterson, P., Landsfeld, M., Pedreros, D., Verdin, J., Shukla, S., Husak, G., Rowland, J., Harrison,
413 L., Hoell, A. and Michaelsen, J.: The climate hazards infrared precipitation with stations—a new environmental
414 record for monitoring extremes, *Scientific Data*, 2, 150066, doi:10.1038/sdata.2015.66, 2015.

415 Guan, K., Good, S. P., Caylor, K. K., Sato, H., Wood, E. F. and Li, H.: Continental-scale impacts of intra-
416 seasonal rainfall variability on simulated ecosystem responses in Africa, *Biogeosciences*, 11(23), 6939–6954,
417 doi:10.5194/bg-11-6939-2014, 2014.

418 Herman, A., Kumar, V. B., Arkin, P. A. and Kousky, J. V.: Objectively determined 10-day African rainfall
419 estimates created for famine early warning systems, *International Journal of Remote Sensing*, 18(February),
420 2147–2159, doi:10.1080/014311697217800, 1997.

421 Herrmann, S. M., Anyamba, A. and Tucker, C. J.: Recent trends in vegetation dynamics in the African Sahel
422 and their relationship to climate, *Global Environmental Change*, 15(4), 394–404,
423 doi:10.1016/j.gloenvcha.2005.08.004, 2005.

424 Houerou, H. Le: Rain use efficiency: a unifying concept in arid-land ecology, *Journal of Arid Environments*,
425 7(3), 213–247, 1984.

426 Huber, S., Fensholt, R. and Rasmussen, K.: Water availability as the driver of vegetation dynamics in the
427 African Sahel from 1982 to 2007, *Global and Planetary Change*, 76(3–4), 186–195,
428 doi:10.1016/j.gloplacha.2011.01.006, 2011.

429 Jönsson, P. and Eklundh, L.: TIMESAT—a program for analyzing time-series of satellite sensor data,

430 Computers & Geosciences, 30, 833–845, 2004.

431 Kaspersen, P. S., Fensholt, R. and Huber, S.: A spatiotemporal analysis of climatic drivers for observed
432 changes in Sahelian vegetation productivity (1982–2007), *International Journal of Geophysics*, 2011, 1–14,
433 doi:10.1155/2011/715321, 2011.

434 Kharin, V. V., Zwiers, F. W., Zhang, X. and Hegerl, G. C.: Changes in temperature and precipitation extremes
435 in the IPCC ensemble of global coupled model simulations, *Journal of Climate*, 20(8), 1419–1444,
436 doi:10.1175/JCLI4066.1, 2007.

437 Lebel, T. and Ali, A.: Recent trends in the Central and Western Sahel rainfall regime (1990–2007), *Journal of*
438 *Hydrology*, 375(1), 52–64, doi:10.1016/j.jhydrol.2008.11.030, 2009.

439 Leisinger, K. M. and Schmitt, K.: *Survival in the Sahel: An ecological and developmental challenge*,
440 International Service for National Agricultural Research, 1995.

441 Liebmann, B., Bladé, I., Kiladis, G. N., Carvalho, L. M. V, Senay, G. B., Allured, D., Leroux, S. and Funk,
442 C.: Seasonality of African precipitation from 1996 to 2009, *Journal of Climate*, 25(12), 4304–4322,
443 doi:10.1175/JCLI-D-11-00157.1, 2012.

444 Mbow, C., Fensholt, R., Rasmussen, K. and Diop, D.: Can vegetation productivity be derived from greenness
445 in a semi-arid environment? Evidence from ground-based measurements, *Journal of Arid Environments*, 97, 56–
446 65, doi:10.1016/j.jaridenv.2013.05.011, 2013.

447 Muggeo, V. M. R.: Estimating regression models with unknown break-points, *Statistics in Medicine*, 22(19),
448 3055–3071, doi:10.1002/sim.1545, 2003.

449 Nicholson, S. E.: The nature of rainfall variability over Africa on time scales of decades to millenia, *Global*
450 *and Planetary Change*, 26(1–3), 137–158, doi:https://doi.org/10.1016/S0921-8181(00)00040-0, 2000.

451 Olsson, L., Eklundh, L. and Ardö, J.: A recent greening of the Sahel—trends, patterns and potential causes,
452 *Journal of Arid Environments*, 63(3), 556–566, doi:10.1016/j.jaridenv.2005.03.008, 2005.

453 Panthou, G., Vischel, T. and Lebel, T.: Recent trends in the regime of extreme rainfall in the Central Sahel,
454 *International Journal of Climatology*, 34(15), 3998–4006, doi:10.1002/joc.3984, 2014.

455 Penning de Vries, F. W. T. and Djiteye, M. A.: The productivity of Sahelian rangeland: a study of soils,
456 vegetation and the exploitation of this natural resource, Centre for Agricultural Publishing and Documentation,
457 Wageningen, Netherlands, 1982.

458 Prince, S., Colstoun, D. and Brown, E.: Evidence from rain-use efficiencies does not indicate extensive
459 Sahelian desertification, *Global Change Biology*, 4(4), 359–374, doi:10.1046/j.1365-2486.1998.00158.x, 1998.

460 Proud, S. R. and Rasmussen, L. V.: The influence of seasonal rainfall upon Sahel vegetation, *Remote Sensing*
461 *Letters*, 2(3), 241–249, doi:10.1080/01431161.2010.515268, 2011.

462 Ratzmann, G., Gangkofner, U., Tietjen, B. and Fensholt, R.: Dryland vegetation functional response to altered
463 rainfall amounts and variability derived from satellite time series data, *Remote Sensing*, 8, 1026,
464 doi:10.3390/rs8121026, 2016.

465 Rishmawi, K., Prince, S. and Xue, Y.: Vegetation Responses to Climate Variability in the Northern Arid to
466 Sub-Humid Zones of Sub-Saharan Africa, *Remote Sensing*, 8(11), 910, doi:10.3390/rs8110910, 2016.

467 R Team.: R: A language and environment for statistical computing. Vienna, Austria: R Foundation for
468 Statistical Computing, <http://www.R-project.org/>, 2014.

469 Romankiewicz, C., Doevenspeck, M., Brandt, M. and Samimi, C.: Adaptation as by-product: Migration and
470 environmental change in Nguith, Senegal, *Journal of the Geographical Society of Berlin*, 147(2), 95–108,
471 doi:10.12854/erde-147-7, 2016.

472 Sanogo, S., Fink, A. H., Omotosho, J. A., Ba, A., Redl, R. and Ermert, V.: Spatio-temporal characteristics of
473 the recent rainfall recovery in West Africa, *International Journal of Climatology*, 35(15), 4589–4605,
474 doi:10.1002/joc.4309, 2015.

475 Smith, M. D.: The ecological role of climate extremes: Current understanding and future prospects, *Journal of*

476 Ecology, 99(3), 651–655, doi:10.1111/j.1365-2745.2011.01833.x, 2011.

477 Taylor, C. M., Belušić, D., Guichard, F., Parker, D. J., Vischel, T., Bock, O., Harris, P. P., Janicot, S., Klein,
478 C. and Panthou, G.: Frequency of extreme Sahelian storms tripled since 1982 in satellite observations, Nature,
479 544(7651), 475–478, doi:10.1038/nature22069, 2017.

480 Thomey, M. L., Collins, S. L., Vargas, R., Johnson, J. E., Brown, R. F., Natvig, D. O. and Friggens, M. T.:
481 Effect of precipitation variability on net primary production and soil respiration in a Chihuahuan Desert
482 grassland, Global change biology, 17(4), 1505–1515, doi:10.1111/j.1365-2486.2010.02363.x Effect, 2011.

483 Wessels, K., Prince, S., Malherbe, J. and Small, J.: Can human-induced land degradation be distinguished
484 from the effects of rainfall variability? A case study in South Africa, Journal of Arid Environments, 68(2), 271–
485 297, doi:10.1016/j.jaridenv.2006.05.015, 2007.

486 Wood, S.: Package mgcv, <https://cran.r-project.org/web/packages/mgcv/index.html>, 2017.

487 Zhang, W., Brandt, M., Guichard, F., Tian, Q. and Fensholt, R.: Using long-term daily satellite based rainfall
488 data (1983–2015) to analyze spatio-temporal changes in the sahelian rainfall regime, Journal of Hydrology, 550,
489 427–440, doi:10.1016/j.jhydrol.2017.05.033, 2017.

490

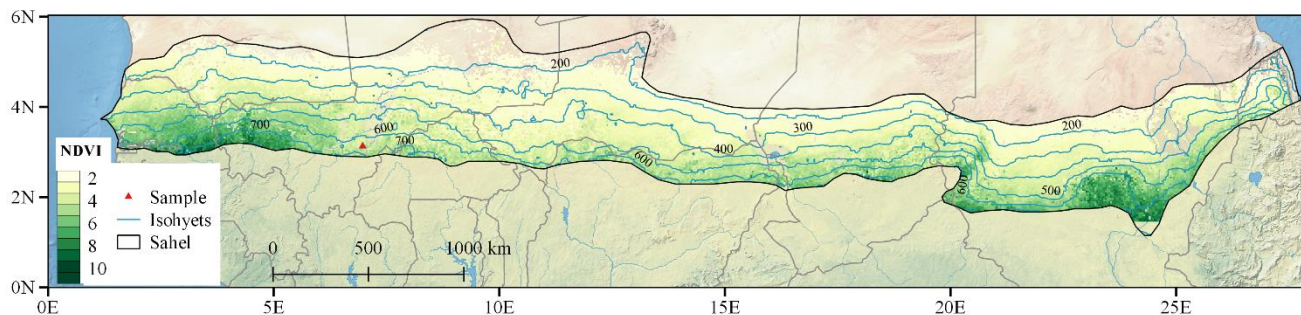
491

Table 1 Rainfall metrics describing the seasonality and extreme events

Index name	Definitions	Units
Onset of wet season (Onset)	The minimum value in the accumulative anomaly of daily rainfall	day of year
Cessation of wet season (Cessation)	The maximum value of the accumulative anomaly of daily rainfall	day of year
Rainy days (RD)	Number of days with rainfall ≥ 1 mm between the onset and the cessation of the wet season	days
Rainfall intensity (SDII)	Ratio of annual total rainfall and number of rainy days ≥ 1 mm	mm day ⁻¹
Heavy rainfall events (R95sum):	Fraction of annual rainfall events exceeding the (2001–2015) 95th percentile	%
Consecutive dry days (CDD):	Maximum number of consecutive days with rainfall < 1 mm during wet season	days

492

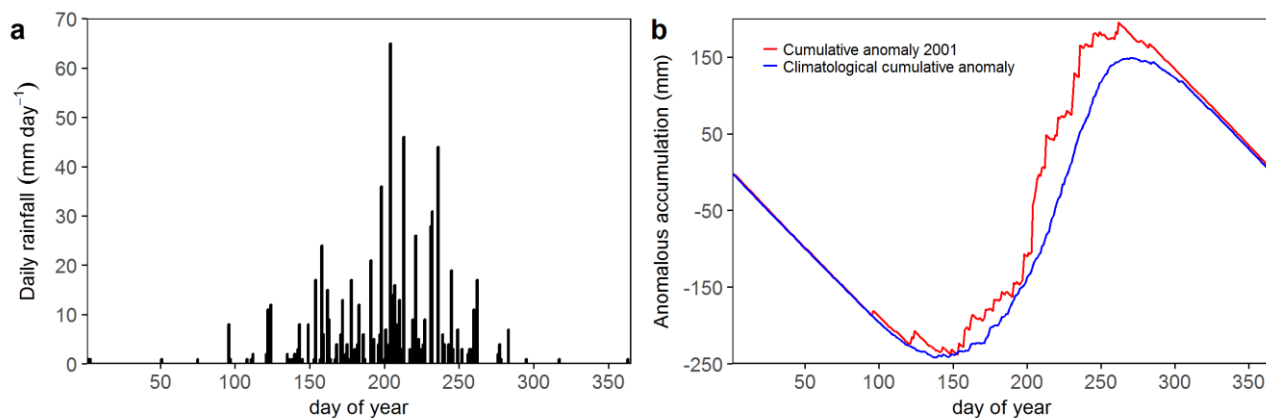
493



494

495 Fig 1. Study area outlining the Sahelian region (black color; 100–800 mm yr⁻¹). Σ NDVI (seasonal integral) is based on a 15
 496 year (2001–2015) average using MODIS data; the red grid point (13.5° N, 5.0° W) is used to illustrate the extractions of onset
 497 and cessation of the wet season shown in Figure 2. Isohyets are based on a 15 year (2001–2015) average of the seasonal
 498 rainfall amount (CHIRPS v2.0).

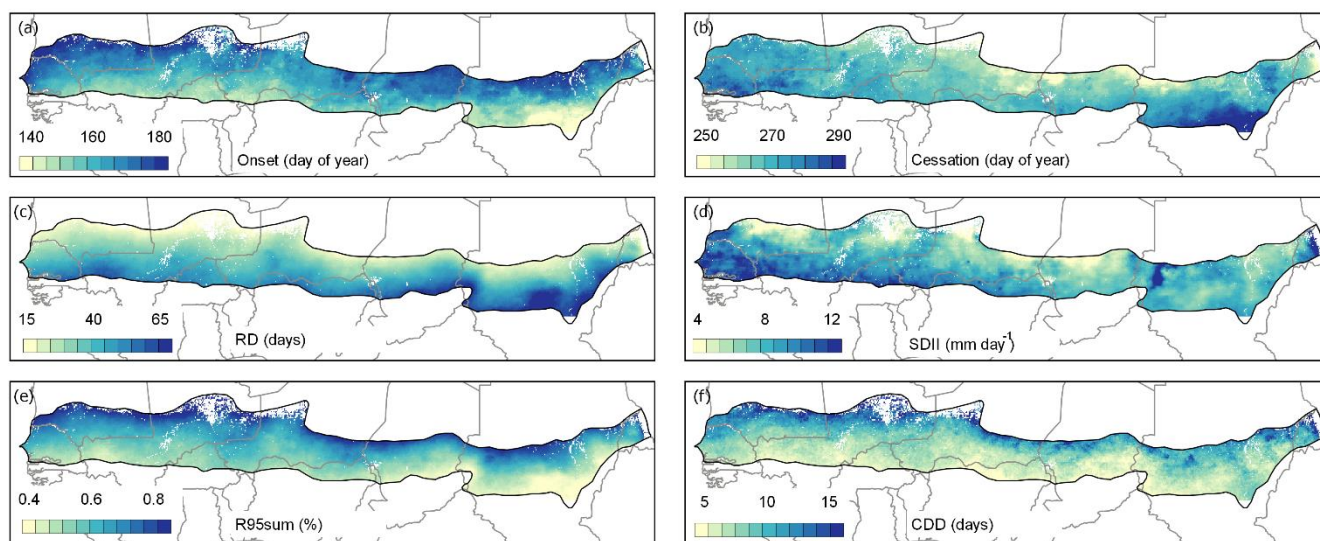
499



500

501 Fig. 2. (a) Daily rainfall distribution and (b) anomalous accumulative curve for the grid point 13.5° N, 5.0° W (shown in Fig.
 502 1) for the year of 2001. The blue line (accumulated anomaly) is computed from a 15 year (2001–2015) average of daily rainfall.

503



505

506

Fig. 3. Spatial distribution of average seasonal rainfall metrics a) onset of wet season (day of year); b) cessation of wet season

507

(day of year); c) rainy days (days); d) daily intensity (mm day^{-1}); e) heavy rainfall events (%); f) consecutive dry days (days)

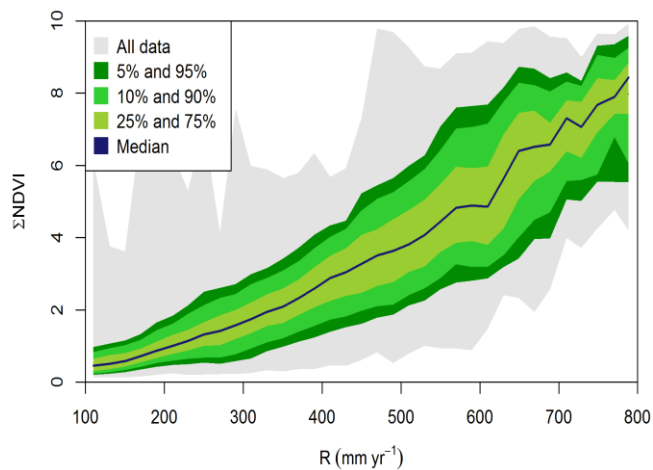
508

based on 15 year averages (2001–2015). Pixels within the study area are masked (white color) in accordance with the

509

description in the methods section.

510

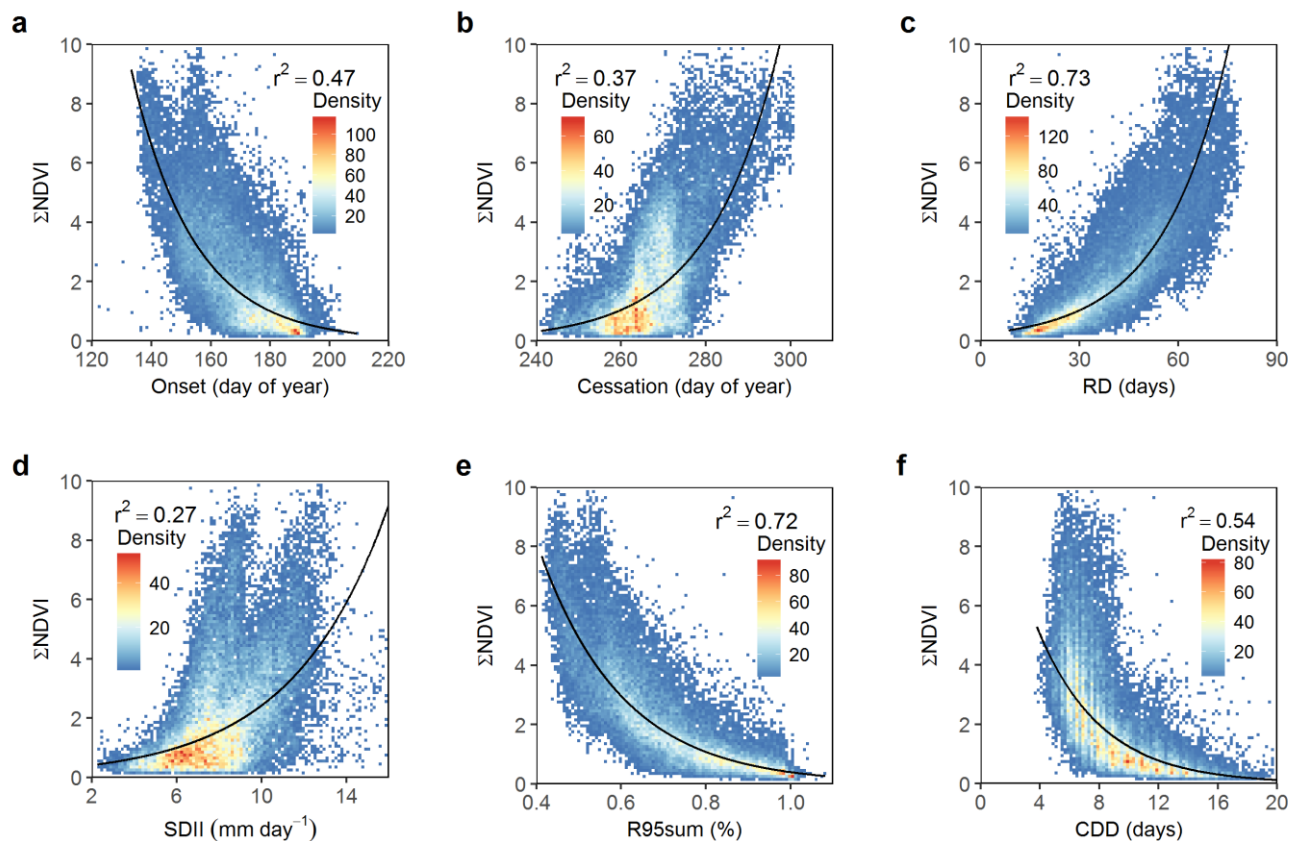


511

512 Fig. 4. Growing season ANPP (Σ NDVI) as a function of mean seasonal rainfall amount (R) plotted as quantiles for the Sahel-
513 Sudanian zone (pixel averages for 2001–2015).

514

515



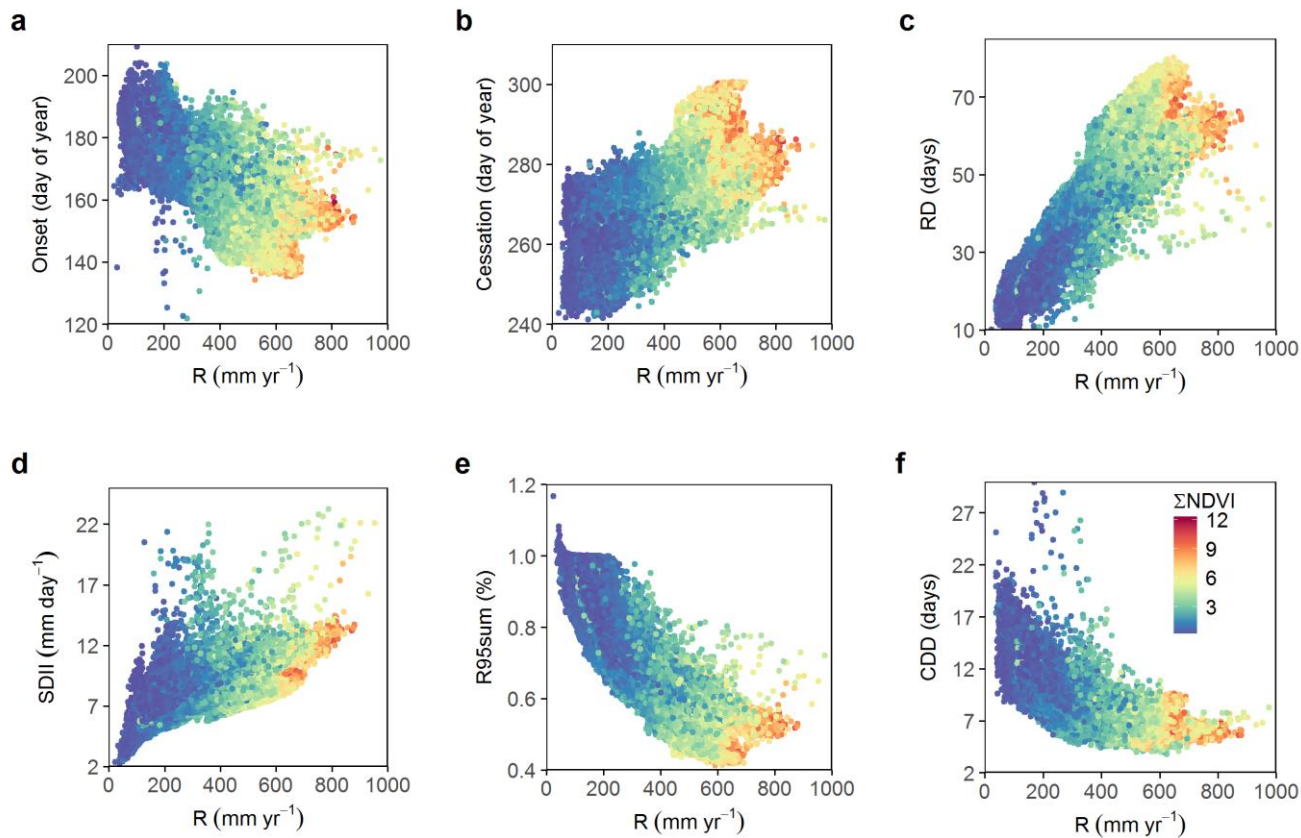
516

517 Fig. 5. Density scatterplot showing the relationships between seasonal rainfall metrics and growing season ANPP (Σ NDVI).
518 All analyses are based on 15 year averages (2001–2015). The black lines are exponential regression curves. All points ($n =$
519 30862) are located between 100 and 800 mm annual rainfall.

520

521

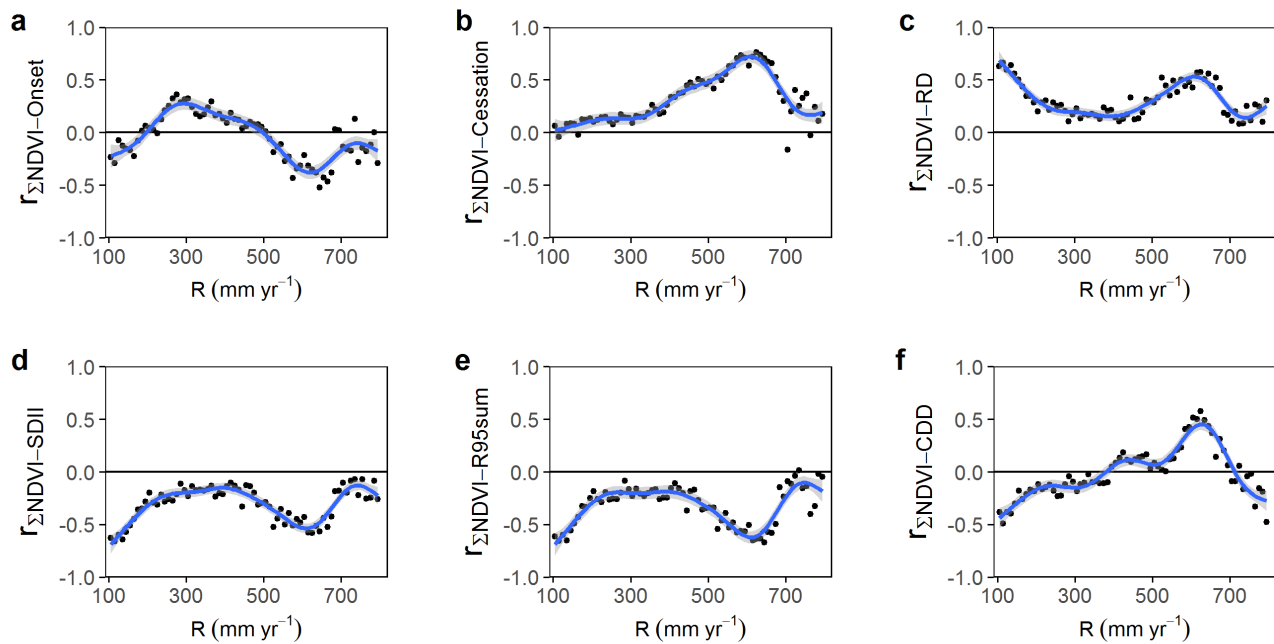
522



523

524 Fig. 6. Relationships between seasonal rainfall metrics and growing season ANPP as a function of seasonal rainfall amount
 525 based on 15 year averages (2001–2015).

526



527

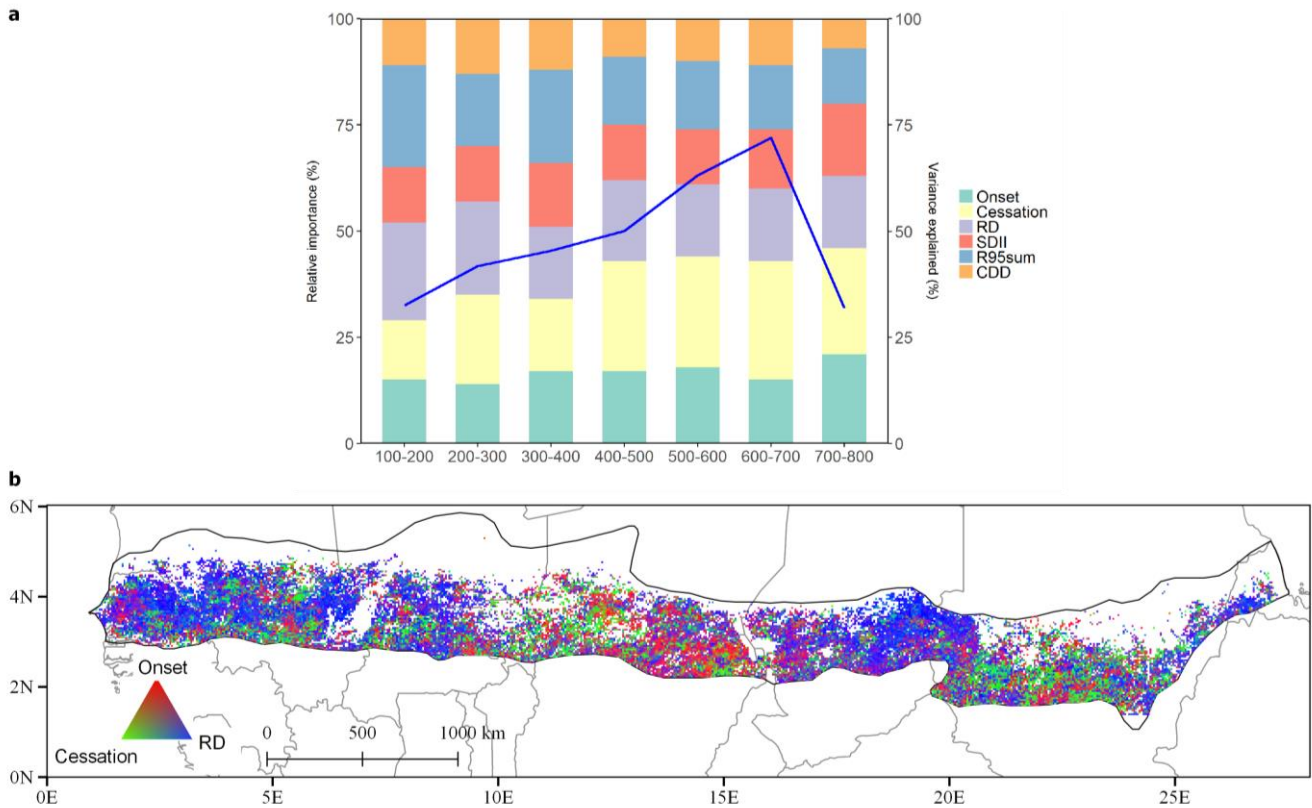
528 Fig. 7. Effects of seasonal rainfall metrics on growing season ANPP as a function of seasonal rainfall amount. The non-

529 parametric Spearman's rank correlation between growing season ANPP and rainfall metrics are shown for each 10 mm interval.

530 The lines are GAM fitting curves and shading represents the 95% confidence intervals of the fitting.

531

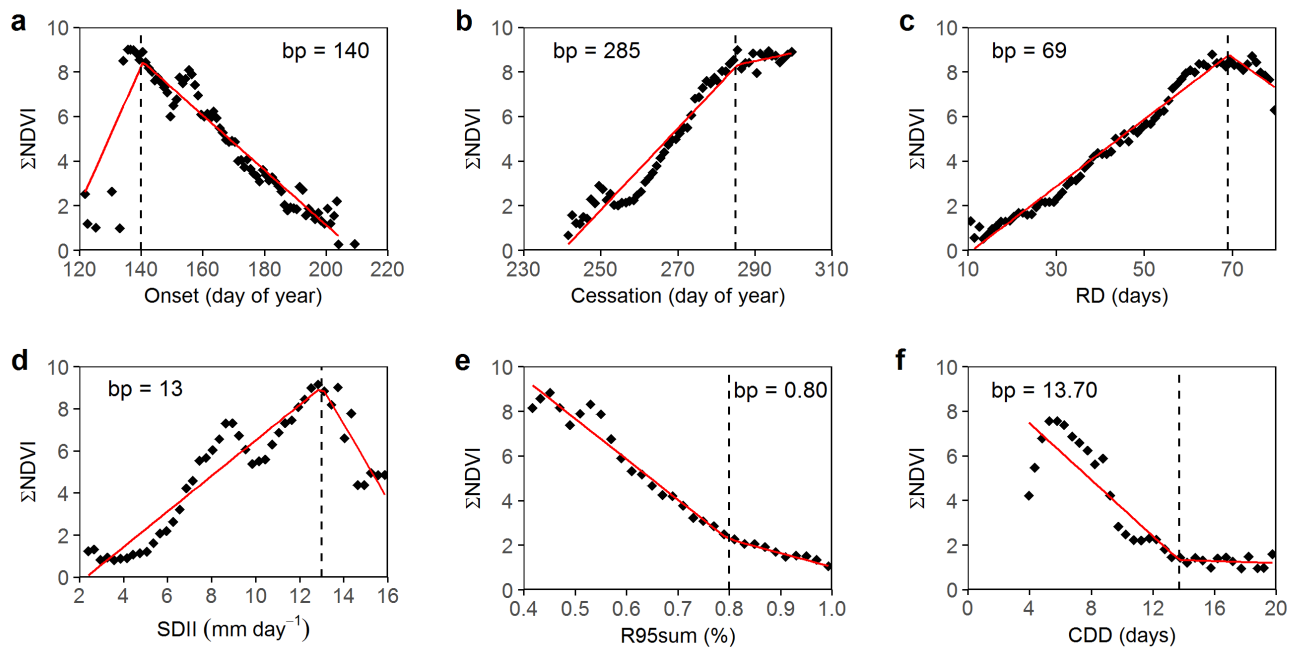
532



533

534 Fig. 8. a) Generalized relationships between growing season ANPP and Onset, Cessation, RD, SDII, R95sum, CDD as a
 535 function of seasonal rainfall amount (100 mm intervals) based on 15 year average values (relative importance in %). The blue
 536 line shows the overall variance of growing season ANPP explained by the rainfall metrics per 100 mm seasonal rainfall amount
 537 based on the random forest method. b) Spatial distribution of the relative importance of onset, cessation of wet season and rainy
 538 days to growing season ANPP for 2001–2015 based on a multiple regression. Pixels within the study area are masked (white
 539 color) in accordance with the description in the methods section.

540



541

542 Fig. 9. Growing season ANPP (individual points represent 95th percentile of Σ NDVI value for each seasonal rainfall metric
 543 bins) plotted against rainfall metrics. Solid red lines denote piecewise regression between growing season ANPP and seasonal
 544 rainfall metrics and dashed lines indicate the breakpoint (bp) for rainfall individual metrics.

545